Improvements to the analytical protocol of lapis lazuli provenance: first study on Myanmar samples.

The European Physical Journal Plus

Improvements to the analytical protocol of lapis lazuli provenance: first study on Myanmar rock samples

--Manuscript Draft--

Manuscript Number:	
Full Title:	Improvements to the analytical protocol of lapis lazuli provenance: first study on Myanmar rock samples
Article Type:	FP: Past and Present: Recent Advances in the Investigation of Ancient etc
Section/Category:	Experimental Physics
Corresponding Author:	Alessandro Re, Ph.D. University of Torino Torino, Torino ITALY
Corresponding Author Secondary Information:	
Corresponding Author's Institution:	University of Torino
Corresponding Author's Secondary Institution:	
First Author:	Gloria Vaggelli
First Author Secondary Information:	
Order of Authors:	Gloria Vaggelli
	Leila Es Sebar
	Alessandro Borghi
	Roberto Cossio
	Alessandro Re, Ph.D.
	Fulvio Fantino
	Alessandro Lo Giudice
Order of Authors Secondary Information:	
Funding Information:	Istituto Nazionale di Fisica Nucleare (IT) (CHNet network) — Not applicable
	Ministero dell'Istruzione, dell'Università e della Ricerca — Not applicable
	Università degli Studi di Torino (NEXTO project) — Not applicable
Abstract:	The study of lapis lazuli is important to find out information about the provenance of a material used since Neolithic Age for the manufacturing of precious carved artefacts. The main sources of lapis lazuli in ancient times are widely considered the Badakhshan deposits in Afghanistan. However, other quarries could have possibly been exploited since antiquity. A protocol to distinguish the provenance of lapis lazuli rocks among four known sources (located in present-day Afghanistan, Tajikistan, Siberia and Chile) by means of non-invasive techniques was set up in the last years. It is based on differences in physical-chemical properties measured in 45 lapis lazuli rocks that constitute our reference database. Recently, samples from the quarry district of Mandalay in Myanmar were supplied by on-site mission. The aim of the present study is to extend the protocol analysing, by means of a multi-analytical approach, 10 rock samples coming from Myanmar to find out significant petrographic and minerochemical markers. Optical microscopy, cathodoluminescence and Scanning Electron Microscopy were used to perform a detailed petrographic and minerochemical characterisation allowing to distinguish the Myanmar lapis lazuli in three main groups.

	SEM-EDX analyses on selected mineralogical phases were performed in order to propose markers useful for the protocol.
Suggested Reviewers:	
Opposed Reviewers:	

Improvements to the analytical protocol of lapis lazuli provenance: first study on Myanmar rock samples

Gloria Vaggelli[(a)], Leila Es Sebar[(b)], Alessandro Borghi[(c)], Roberto Cossio[(c)], Alessandro Re[(b,d)], Fulvio Fantino[(e)] and Alessandro Lo Giudice[(b,d)]

(a) CNR- Isitituto di Geoscienze e Georisorse, Via Valperga Caluso, 35, Torino, Italy

(b) Dipartimento di Fisica, Università di Torino, Via Giuria 1, Torino, Italy;

(c) Dipartimento di Scienze della Terra, Università di Torino, Via Valperga Caluso 35, Torino, Italy;

(d) INFN Sezione di Torino, Via Giuria 1, Torino, Italy;

(e) TecnArt S.r.l., via Modena 58, Torino Italy

*corresponding author: alessandro.re@unito.it

Abstract

The study of lapis lazuli is important to find out information about the provenance of a material used since Neolithic Age for the manufacturing of precious carved artefacts. The main sources of lapis lazuli in ancient times are widely considered the Badakhshan deposits in Afghanistan. However, other quarries could have possibly been exploited since antiquity.

A protocol to distinguish the provenance of lapis lazuli rocks among four known sources (located in present-day Afghanistan, Tajikistan, Siberia and Chile) by means of non-invasive techniques was set up in the last years. It is based on differences in physical-chemical properties measured in 45 lapis lazuli rocks that constitute our reference database.

Recently, samples from the quarry district of Mandalay in Myanmar were supplied by on-site mission. The aim of the present study is to extend the protocol analysing, by means of a multi-analytical approach, 10 rock samples coming from Myanmar to find out significant petrographic and minerochemical markers. Optical microscopy, cathodoluminescence and Scanning Electron Microscopy were used to perform a detailed petrographic and minerochemical characterisation allowing to distinguish the Myanmar lapis lazuli in three main groups.

SEM-EDX analyses on selected mineralogical phases were performed in order to propose markers useful for the protocol.

Key Words: archaeometry, lapis lazuli, SEM-EDX electron microprobe, lazurite, Myanmar, provenance

1. Introduction

Lapis lazuli is a semi-precious blue stone. It was used as decorative material by ancient civilizations since Neolithic Age (VII millennium BC) for the manufacturing of precious carved artefacts [1]. Despite its extensive employment in palaces, temple and tombs, the knowledge on the provenance of this rock is still incomplete. The possibility to associate the raw material to man-made objects could be helpful to reconstruct trade routes in specific historical periods.

The wide employment of lapis lauzuli is related to its unique blue colour which is due to the occurrence of lazurite: a sulphur-bearing member of the sodalite group which can be also defined as sulphur-bearing haüyne (in the past lazurite was considered a variety of haüyne rich in sulphur [2-3] containing both sulfate and sulfide sulphur).

Lapis lazuli is generically classified as a metamorphic rock, even if this definition could not be considered exhaustive, due to the complexity of mechanisms involved in its genesis.

Due to the low probability of geological conditions in which it can be formed, only few sources of lapis lazuli exist in the world [4-5]. In antiquity just one source, the Sar-e-Sang deposits in the Badakhshan Region, in present-day Afghanistan, seems to have supplied the whole of the Middle East, South Asia and Central Asia civilizations, among which particularly Indus Valley, Syro-Mesopotamian and ancient Egyptian civilization can be considered [6-10].

However, the early exploitation of the other geologically documented sources in the area as in Lyadzhuar Dara (Pamir Mountains in present-day Tajikistan) and in Swat Valley (present-day Pakistan), or in more distant Asian regions, even if less probable, as in Irkutsk (near Lake Baikal, present-day Siberia) and in Mogok (Mandalay Region, present-day Myanmar), could be considered ([11-12] and references therein). In particular, geographical considerations (great distance from ancient civilization sites, arduous terrains, etc.) are not valid criterions to exclude alternative sources of lapis lazuli in ancient time, especially because knowledge of early trade routes in this area is still largely incomplete. Moreover, other Asian lapis lazuli sources are described in ancient written testimonies, but their existence has not yet been proved as for example Iranian sources [7].

About geologically documented sources, they were reported in literature only in recent times and possibly exploited only in the last centuries, although it cannot be excluded that they were exploited in some historical periods and later forgotten. Among them the Siberian sources, not currently exploited, could be considered for the historical importance of some of their deposits even if in a different period of time. They played a crucial role especially from 18th century, period in which other attribution issue and questions of historical importance could arise. In fact, in this period the production of remarkable pieces of art confirm a dynamic background in the hard stones manufacturing.

To solve the determination of lapis lazuli origin by means of an analytical approach in 2008, a long-term research, involving an interdisciplinary team, was started in Turin (Italy) [12-17].

In order to achieve the purpose of a complete characterization of the rock, a multi-technique approach was adopted, including both invasive and non-invasive techniques, by means of bench-top-instruments and large scale facilities [18]. The analytical techniques applied were mainly: optical microscopy, Scanning Electron Microscopy with Energy-Dispersive X-ray spectrometry (SEM-EDX) for major elements identification, micro-beam Particle Induced X-ray Emission (μ-PIXE) and micro-beam X-Ray Fluorescence (μ-XRF) for trace elements identification, and finally cathodoluminescence (CL) and micro-beam IonoLuminescence (μ-IL) to characterize the luminescence properties. Being lapis lazuli a very heterogeneous material, the analyses were focused on the single mineral phases to identify minero-chemical markers.

Until now, 45 lapis lazuli rocks of known provenance from 4 quarry districts (fig. 1) have been analysed, creating a large database. The database [12] is composed by 21 samples from Badakhshan in Afghanistan; 4 samples from Liadjura-Dara, Pamir Mountains in Tajikistan; 11 samples from Lake Baikal area in Siberia (4 from Malaya Bistraya quarries and 7 from Sludyanka River quarries) and 9 samples from Coquimbo region in Chile. Chilean deposit was taken into account because samples from this provenance area are easy to find, being currently exploited, and because of its possible exploitation by ancient civilizations of the American continent [19]. In the case of Lake Baikal, a geological expedition was organised to collect samples from two quarries in the area (Malaya Bistraya and Sludyanka River), considering that the mines are no longer exploited and it is difficult to find rocks of recorded provenance. In [12], the protocol used to associate a lapis lazuli rock to one of the four provenances was summarised (fig. 2) and applied to Ancient Egypt artefacts.

It is based on the presence or absence of a mineralogical phase, minor/trace elements occurrence inside a peculiar mineral (in particular diopside and pyrite were taken in account) and the different luminescence of the same mineral. Two kinds of markers were identified: strong markers, which means physical-chemical features are systematically present or absent in all the 45 analysed samples and weak markers, which are features unique for a lapis lazuli quarry district but not observed in all the samples from that provenance. The aim of the present study is to increase the number of information in the rocks database to improve our protocol and to find out other significant either petrographic or minerochemical markers. In particular, for the first time a study was carried out by a multi-analytical approach on 10 rock samples bought in Myanmar (but not georeferenced), which are coming from the quarry district near Mogok in the Mandalay Region (fig. 1), a provenance that was not yet considered in our protocol.

2. Geological settings of lapis lazuli occurrences

The mechanism that lead to lapis lazuli formation is quite complex and still not clear, despite the existence of a large number of studies.

The paragenesis of this rock can consist of many different minerals. In general, the mineral assemblage is characterised by the widespread or localised occurrence of a blue feldspathoid, mostly lazurite [20], together with other mineral inclusions, such as pyrite, calcite, diopside, feldspar and feldspathoid.

Brøgger and Bäckström [21] for the first time suggested that lapis lazuli is a product of contact metamorphism and metasomatism of dolomitic limestones or marbles. Indeed, lapis lazuli is mostly found in limestone or dolostone, interested by contact metamorphism. In these zones the formation of lazurite is possible thanks to the presence of hydrothermal fluxes rich in S, Cl and Na, elements essential to this mineral phase. The lapis lazuli deposit in the Italian Mountain, Colorado [22] and the ones in Coquimbo, Chile [23-25] are an example of this kind of origin.

Instead, the mechanism involved in the lapis lazuli formation is different for the deposits on Baffin Island, Canada [26] and for the famous Badakhshan area, in Afghanistan. In particular, these mines are affected by a regional metamorphism, involving high temperatures and pressures and the processes leadings to lazurite occurrence is still uncertain [27].

In this paper, lapis lazuli samples from the Mogok region (central Myanmar) are studied. The Mogok region is located 120 km north of Mandalay, on the western edge of the Shan upland. The geological structure is defined by its position in the marginal part of the Shan central massif, which is the largest outcrop of Precambrian metamorphic rocks in the Mesozoic Indochina fold belt. A large part of the region is underlain by garnet-sillimanite gneisses and crystalline schists with intercalations of sillimanite quartzites. The Mogok group of gneisses locally contains thick sequence of calcite and dolomite-calcite marbles and calciphyres with associated calcareous diopside gneisses [28].

3. Analytical method

Ten of the twelve available quarry samples from Myanmar (fig. 3) were prepared as thick petrographic section (ca. 100-120 μm thickness) mounted on plexiglass slides. Samples have been carbon-coated to avoid charging effects during SEM-EDX measurements.

At first, optical microscope, CL and SEM were used to perform a detailed petrographic characterisation determining the texture and the mineralogical assemblage of the rock samples and to select the mineral phases to analyse by SEM-EDX electron microprobe.

SEM-EDX measurements were performed in order to determine the chemical composition of the main rock-forming minerals such as lazurite, diopside, amphibole, feldspar and feldspathoid. A Scanning Electron Microscope (JEOL JSM-IT300LV) equipped with an energy-dispersive X-ray spectrometer (EDX), with a SDD (a silicon drift detector from Oxford Instruments), hosted at the Earth Science Department of the University of Torino, was used for the determination of major chemical elements. The common experimental parameters were: accelerating voltage 15 kV, counting time 50 s, process time 5 µs and working distance 10 mm. The measurements were conducted in high vacuum conditions. The EDX acquired spectra were corrected and calibrated both in energy and in intensity thanks to measurements performed on cobalt standard introduced in the vacuum chamber with the samples. The Microanalysis Suite Oxford INCA Energy 200, that enable spectra visualization and elements recognition, was employed. A ZAF data reduction program was used for determining the chemical composition of major elements. The resulting full quantitative analysis is obtained from the spectra, using natural oxides and silicates from Astimex Scientific Limited® as standards. All the analyses, except lazurite, were formula recalculated using the MINSORT computer program of Petrakakis and Dietrich [29].

As regards to lazurite, SEM-EDX measurements were carried out with a defocused electron beam, in order to limit the thermal effect on Na and O. Because very few studies focused on lazurite we adopted the mineral formula suggested in [20]:

$(Na, Ca)_{7.5\text{-}8}(Si, Al)_{12}(O, S)_{24}(SO_4, Cl)_{1.3\text{-}2}$

Hence, the quantification method for the mineral formula calculation, adopted in this work was the following: the lazurite formula was calculated imposing Si+Al = 12 cations and O^{2-}+S^{2-} = 24 anions [20, 30]. The problems connected to sulphur species was resolved as follows: part of the total amount of S was assumed to be S^{2-} replacing O^{2-} in the 24-fold position, whereas the remaining amount was assumed to be SO_4^{2-} in the position occupied by sulphate and chlorine. It is worth highlighting that this assumption is improper considering the crystallographic structure of the mineral, nevertheless it does not affect in relevant way the calculated stoichiometry, exclusively employed for the cations recalculation in order to verify contingent information linked to the provenance from differences in chemical composition.

4. Results and Discussion

4.1 Petrography

The main mineral assemblage of the studied Myanmar lapis lazuli are represented by diopside, amphibole, lazurite, and calcite and as accessory mineral by apatite and pyrite. However, according

to differences in mineral abundances, it is possible to distinguish two main groups: i) the samples characterised by the abundant presence of amphibole generally associated to lazurite and diopside and ii) the samples characterised by the amphibole-absence with a lazurite-diopside-calcite association; in this last group two subgroups can be identified, by the presence or the absence of nepheline-haüyne-plagioclase association. For each sample, some significant back-scattering electrons (BSE) images for some identified phases are reported in fig.4, whereas the whole mineral assemblage for each sample is shown in Table 1. The mineral abbreviations used in fig. 4 are the same as in [31]. As shown in Table 1 the paragenesis and petrographic features observed allow to well discriminate among the Myamar rock groups, by the presence or absence of amphibole-group minerals and by the presence of nepheline-haüyne-plagioclase association (gray boxes).

In comparison with other provenance, the presence of diopside as a main mineralogical phase of Myanmar source confirm the possibility expressed in the protocol to distinguish Asian lapis lazuli from Chilean ones that are poor in this mineral and rich in wollastonite. Moreover, the observed pyrite crystals, although smaller and in minor quantity than in other provenances, are well formed contrarily to the Siberian one that present an altered form with the presence of iron-hydroxide minerals, showing an intensive compositional zoning in which sulphur-free zones prevail.

4.1.1 The amphibole-bearing group

The samples characterised by the abundant presence of a mineral phase belonging to the amphibole-group are: MYA02, MYA03, MYA04, MYA06. They show a porphyritic texture defined by diopside phenocrystals surrounded by a fine grain groundmass of lazurite and amphibole-group minerals with a medium-fine grain size (fig. 4a), possibly reflecting their simultaneous intergrowth at eutectic point during the cooling of a magmatic process. Sometimes, diopside and amphibole grew as large crystals (mm in grain size) characterized by a rim of lazurite at their contact (fig. 4b). In this group pyrite, apatite, calcite, pitchblende and sodalite occur as accessory minerals.

4.1.2 Amphibole-absence with lazurite-diopside-calcite association group

As previously pointed out two subgroups of the lazurite-diopside-calcite are described according to the presence or absence of the association nepheline-haüyne-plagioclase.

The MYA07, MYA08, MYA09 samples belong to the subgroup without nepheline-haüyne-plagioclase. These samples show a medium fine grain size with a porphyritic texture; diopside occurs in large veins or coarse crystals in association with calcite (fig. 4c). The diopside-calcite association is surrounded by a ground mass in which at higher magnification a fine mixture of lazurite and diopside can be distinguished. Apatite, pitchblende, pyrite, chalcocite, sphalerite and kaolinite are

observed as accessory minerals with decreasing order of abundance.

The MYA10 and MYA11 samples belong to the subgroup with the nepheline-haüyne-plagioclase association. The diopside crystals (from hundred μm up to 1 mm) appear in large veins or as a coarse assembled grain surrounded by a groundmass consisting either in a fine mixture of nepheline and albite or of lazurite, haüyne and nepheline (fig. 4d). The unmixed structure between nepheline and albite reflects a simultaneous intergrowth at eutectic point during the cooling of a magmatic mass. The presence of apatite and pyrite, is observable in both samples. Other accessory minerals are sodalite, phlogopite and scapolite.

The MYA12 sample is placed in this group but a separate description is necessary; indeed, part of the sample consists of a large vein, crosscutting the common mineral assemblage. In the host rock the diopside-calcite association is surrounded by a ground mass in which at higher magnification a fine mixture of lazurite and diopside can be distinguished (fig. 4e). In the vein the paragenesis consist of lazurite, K-feldspar, quartz, diopside. In particular, the quartz shows a coronitic rim of K-feldspar and it is never directly in contact with lazurite (fig. 4f). The presence of apatite, pitchblende and opaque minerals can be observed, too, together with cordierite and phlogopite.

4.2 Mineral chemistry

Electron microprobe analyses by means of SEM-EDX technique were performed on some of the main rock-forming minerals: diopside, lazurite, and amphibole, as well as on a selection of accessory minerals as feldspars. Results have been compared, for discriminative porpoises, with those reported in literature by [20, 26, 32].

4.2.2 Diopside

Diopside ($CaMgSi_2O_6$) is a rock-forming silicate belonging to the monoclinic pyroxene series and forming a complete solid solution with hedenbergite ($CaFeSi_2O_6$). Representative electron microprobe analyses and calculated parameters on compositional diagram of pyroxene [33] (wollastonite, enstatite, ferrosilite and jadeite) are reported in Table 2. All the data subdivided by sample are shown in fig. 5, where each point represents an individual measurement. The significant statistics for this mineral phase contribute to take into account the variability in element contents also within the same sample. Data shows a good linear dispersion that indicate the substitution of Ca and Mg with Na and Al. It is worth to notice (fig.5) that the higher values of Na and Al (maximum 0.15 and 0.18 atoms p.f.u., respectively) correspond to lower Mg and Ca contents and can be linked to a partial substitution of diopside with the jadeitic end member, suggesting the occurrence of metamorphism phenomena. Indeed, diopside ($CaMgSi_2O_6$) can be replaced under metamorphic

conditions by jadeite end member ($NaAlSi_2O_6$), a pyroxene variety stable at high P-T conditions in metamorphosed granitoid according to the reaction Albite + Quartz = Jadeite. This substitution is directly proportional to the pressure conditions of recrystallization [34], in particular Ca and Mg are replaced by Na and Al, respectively, to maintain the balance of the charge according to the following scheme: Na + Al = Ca + Si. Despite the high variability of element contents in diopside crystals of the same samples, it is possible to observe in fig. 5 different degree of metamorphic overprinting on the basis of the proposed petrographic grouping. Amphibole-bearing group, i.e MYA02, MYA03, MYA04 and MYA05 (orange-red points in fig. 5) and in particular MYA02 and MYA03 have a low content of Na and Al that may suggest a magmatic origin. On the contrary, samples belonging to the subgroup with the nepheline-haüyne-plagioclase association (MYA10 and MYA11, green points in fig. 5) seem to have the higher metamorphic imprint.

Results on diopside from other provenance reported in literature [13, 20, 26] show a similar linear dispersion when Na and Mg (a.p.f.u.) are plotted versus Ca and Al (a.p.f.u.), respectively, mainly overlapping to data in fig. 5. However, Tajikistan and Afghanistan samples show an average higher amount of Na and Al respect to Myanmar diopside, implying a major jadeite substitution whereas Siberian diopside show an average lower amount of Na and Al reflecting a minor grade of metamorphism [13].

4.2.1 Lazurite

Lazurite, a deep blue to greenish blue mineral, is a sulphur-bearing member of the sodalite group, whose ideal chemical formula is $Na_6Ca_2Al_6Si_6O_{24}S_2$

Representative quantitative analyses of lazurite from Myanmar lapis lazuli are reported in Table 3. The chemical composition of lazurite shows that Si content is in the range 6.00-6.20 atoms per formula unit (a.p.f.u.), with Al content in the range 5.80-6.00 a.p.f.u.. A wider dispersion is shown by Na content (ranging between 6.5-7.6 a.p.f.u.) showing a weak linear correlation with Ca content (ranging between 0.7 - 1.2 a.p.f.u.). Samples MYA12 is Ca richer and form a distinct data group (fig. 6). Even if a grouping could be observed, no evident correlation exists between the three groups identified on a petrographic basis and the chemical composition of the relative lazurites.

In fig. 7 results on lazurite have been compared, for discriminative purposes, with those reported in literature by [20, 26, 32]. In particular, in [20] are listed the major element contents for two samples from Myanmar (purple triangles in fig. 7) that are in good agreement with data obtained in this work (purple circles in fig. 7). Despite the high number of points measured compared to other provenances, data from Myanmar are less dispersed than other provenances; this behaviour could be attributed to a more homogeneous composition of the lazurite from this provenance independently from the

proposed petrographic grouping. Myanmar samples plot in a well-defined field, showing only a small overlapping with Baffin Island and other Asian data. Particularly, most of the Myanmar lazurite are Na-richer and Ca-poorer than the other provenances. If confirmed by means of a more significative statistics on other provenances this feature could be added to our protocol at least as a weak marker.

4.3 Amphibole

As reported in the petrography section, amphiboles only occur in a specific group in association with lazurite (MYA02, MYA03, MYA04, MYA06). According to the new classification and nomenclature scheme for the amphibole suggested by Hawthorne et al. [35] the analysed amphibole belongs to the calcium supergroup (i.e. $^{B}Ca/^{B}[Ca + Na] \geq 0.75$) with an edenite-pargasite composition (fig. 8a; Table 4). Data referring to MYA02 and MYA03 samples are more clustered than the others. Finally, fig. 8b shows the chemical variation of the Ca-rich amphiboles as ($[Al]^{VI} + Fe^{3+} + Ti$) vs $[Al]^{IV}$ values expressed as atoms per formula unit. The compositions are intermediate between the two end member tremolite and pargasite, with prevalent edenite type substitution ($\square_{[A]} + Si = Na_{[A]} + [Al]^{IV}$, respect to the tschermakite substitution ($Si + Mg = [Al]^{IV} + [Al]^{VI}$).

As regards to amphibole the occurrence of this phase is quite useful for discriminative porpoises and the minerochemical description is significantly necessary because it is rarely reported in literature. In the other 45 samples of our database it was never observed as main mineralogical phase. In literature, in [24] is reported the occurrence of tremolite and hedenbergite from the lapis lazuli deposit of Flor de los Andes (Chile). Tremolite occurrence in the Badakhshan deposits are reported also in [36-37]. Moreover, in [32] is reported the presence of amphibole in the Afghanistan lapis lazuli.

4.4 Other minerals

Other mineral phases were found and analysed in this set of samples: feldspars, nepheline, phlogopite, cordierite, sodalite, muscovite. A brief chemical description of the main features of feldspars observable in sample MYA10, MYA11 e MYA12, which represent common rock-forming minerals, is reported. The analyses carried out on feldspars by means of SEM-EDX are represented in Table 5. The feldspar formula was calculated imposing the number of Oxygen atoms equal to 8 anions.

Plagioclase with an albite/oligoclase, composition occur in MYA10 and MYA11 samples, corresponding to the diopside-lazurite with nepheline group. K-feldspar occurs in association with quartz in the vein of MYA12 which represent an unusual sample (see petrography section).

As regards to alkali feldspar and plagioclase the occurrence of oligoclase and albite is observable in

MYA10 and MYA11, whereas K-feldspar is a characteristic of MYA12.

6. Conclusions

In this work, to extend the provenence protocol related to four known sources (located in present-day Afghanistan, Tajikistan, Siberia and Chile) ten lapis lazuli quarry samples from the district of Mandalay in Myanmar were studied by means of a multi-analytical approach. To the best of our knowledge, the number of analysed samples largely increase the data found in literature.

A detailed petrographic and minerochemical characterisation was carried out on the rock samples and the texture and the mineralogical assemblage were determined. The lazurite-diopside association and the presence of nepheline or amphiboles in addition to pyrite and other accessory minerals allowed to distinguishing the Myanmar lapis lazuli in three main groups with different metamorphic overprinting. The presence of diopside as a main mineralogical phase of Myanmar source confirms the possibility expressed in the protocol (fig. 2) to distinguish Asian lapis lazuli from Chilean ones that are poor in this mineral and rich in wollastonite. Moreover, the pyrite crystals in Myanmar rocks are stable contrarily to the Siberian one, which present an altered form. This result confirms that part of the second step of the protocol can be applied also on Myamar samples to distinguish them from Siberian one. Results by means of SEM-EDX on major element contents in lazurite compared with data in literature are promising, at least as "weak maker", to distinguish this provenance from Tajikistan and Afghanistan rocks.

Acknowledgement

This work was financially supported by Ministero dell'Istruzione, dell'Università e della Ricerca (M.I.U.R), by the NEXTO project (Progetti di Ateneo 2017) and by the INFN-CHNet network. The authors warmly thank Prof. Luca Martire (Earth Science Department, University of Torino) for the availability of his cathodoluminescence apparatus.

Table Captions

Table 1. Summary of the mineral phases identified for each sample (in bolt the main mineralogical phases). The paragenesis and petrographic features observed allow to well discriminate among the groups (gray boxes), by the presence or absence of amphibole- group minerals and by the presence of nepheline - hauyna - plagioclase association.

Table 2. Representative SEM-EDX analyses of pyroxene calculated on the basis of 6 atoms of Ox. bld: below detection limit. Pyroxene end-members (Total Sum = 1): wo = wollastonite; fs = ferrosilite; en = enstatite; jd = jadeite.

Table 3. Representative SEM-EDX analyses of lazurite calculated imposing Si+Al = 12 cations and $O^{2-}+S^{2-}$ = 24 anions.

Table 4. Representative SEM-EDX analyses of amphibole calculated on the basis of 23 atoms of Ox. bld: below detection limit.

Table 5. Representative SEM-EDX analyses of feldspars calculated on the basis of 8 atoms of Ox. bld: below detection limit.

Figure Captions

Fig. 1. Map of the geological occurrences of lapis lazuli used in our database: 1) Badakhshan in Afghanistan (21 samples), 2) Liadjura-Dara, Pamir Mountains in Tajikistan (4 samples), 3) Lake Baikal area in Siberia (11 samples), 4) Mandalay Region in Myanmar (12 samples), 5) Coquimbo region in Chile (9 samples).

Fig. 2. Schematic diagram of the protocol proposed to identify the provenance of lapis lazuli among four known sources (published in [12]).

Fig. 3. A representative set of the ten lapis lazuli rock samples from Myanmar. From up to down: MYA03, MYA08, MYA12.

Fig. 4. BSE images of the different typologies of Myanmar samples.

Fig. 5. SEM-EDX analyses of diopside; each point represents an individual measurement. Na vs Al diagram shows a good positive linear dispersion.

Fig. 6. SEM-EDX analyses of lazurite; each point represents an individual measurement. Na vs Ca cation diagram shows a broad negative linear dispersion.

Fig. 7. SEM-EDX discriminative diagrams between lazurite of different provenances, based on major element contents. Literature data are from [20, 26, 32].

Fig. 8. a) Classification diagram for the amphibole according to [35]. b) Al^{IV} vs $Al^{VI} + Fe^{3+} + Ti$ bivariant diagram. The analysed amphibole plot along the edenite - pargasite tie-line.

References

[1] Casanova, M., 2001. Le lapis-lazuli, la pierre précieuse de l'Orientancien. Dialogues d'histoire ancienne 27, 149–170.

[2] Rogers A.F., 1938. Lapis lazuli from San Bernardino County, California. American Mineralogist, 23(2): 111-115

[3] Van Peteghem J.K., Burley B.J., 1963. Studies on solid solution between sodalite, nosean and hauyne. Canadian Mineralogist, 7: 808-813 (*)

[4] Voskoboinikova, N., 1938. The mineralogy of the Slyudyanka deposits of lazurite. Zapiski Vserossiyskogo Mineralogicheskogo Obshchestva 67, 601–622.(*)

[5] Wyart, J., Bariand, P., Filippi, J., 1981. Lapis lazuli from Sar-i-Sang, Badakhshan, Afghanistan. Gems and Gemmology 17, 184–190.

[6] Bulgarelli G.M., Tosi M., 1977. La lavorazione ed il commercio delle pietre semipreziose nelle citta dell'Iran protostorico (3200-1800 a.C.). Geo-Archeologia, Japadre Editore, L'Aquila, 1-2: 37-50

[7] Herrmann, G., 1968. Lapis Lazuli: The Early Phases of Its Trade. Iraq 30, 21.

[8] Herrmann, G., Moorey, P., 1983. Lapis lazuli, in: Reallexikon Der Assyriologie Und Vorderasiatischen Archaologisch. W. de Gruyter, Berlin, pp. 489–492.

[9] Sarianidi, V., Kowalaski, L.H., 1971. The lapis lazuli route in the ancient East. Archaeology 24, 12–15.

[10] Tosi, M., Vidale, M., 1990. 4th Millennium BC Lapis Lazuli Working at Mehrgarh, Pakistan. Paléorient 16, 89–99.

[11] Law, R., 2014. Evaluating potential lapis lazuli sources for ancient South Asia using sulfur isotope analysis. In: Lamberg-Karlovsky CC, Genito B (eds) "My life is like the summer rose" Maurizio Tosi e l'archeologia come modo di vivere. Archaeopress, Oxford, pp. 419–429

[12] Lo Giudice, A., Angelici, D., Re, A., Gariani, G., Borghi, A., Calusi, S., Giuntini, L., Massi, M., Castelli, L., Taccetti, F., Calligaro, T., Pacheco, C., Lemasson, Q., Pichon, L., Moignard, B., Pratesi, G., Guidotti, M.C., 2017. Protocol for lapis lazuli provenance determination: evidence for an Afghan origin of the stones used for ancient carved artefacts kept at the Egyptian Museum of Florence (Italy). Archaeological and Anthropological Sciences 9, 637–651.

[13] Angelici, D., Borghi, A., Chiarelli, F., Cossio, R., Gariani, G., Lo Giudice, A., Re, A., Pratesi, G., Vaggelli, G., 2015. μ-XRF Analysis of Trace Elements in Lapis Lazuli-Forming Minerals for a Provenance Study. Microscopy and Microanalysis 21, 526–533.

[14] Lo Giudice, A., Re, A., Calusi, S., Giuntini, L., Massi, M., Olivero, P., Pratesi, G., Albonico, M., Conz, E., 2009. Multitechnique characterization of lapis lazuli for provenance study. Analytical and Bioanalytical Chemistry 395, 2211–2217.

[15] Re, A., Angelici, D., Lo Giudice, A., Corsi, J., Allegretti, S., Biondi, A.F., Gariani, G., Calusi, S., Gelli, N., Giuntini, L., Massi, M., Taccetti, F., La Torre, L., Rigato, V., Pratesi, G., 2015. Ion Beam Analysis for the provenance attribution of lapis lazuli used in glyptic art: The case of the "Collezione Medicea." Nuclear Instruments and Methods in Physics Research Section B: Beam Interactions with Materials and Atoms 348, 278–284.

[16] Re, A., Angelici, D., Lo Giudice, A., Maupas, E., Giuntini, L., Calusi, S., Gelli, N., Massi, M., Borghi, A., Gallo, L.M., Pratesi, G., Mandò, P.A., 2013. New markers to identify the provenance of lapis lazuli: trace elements in pyrite by means of micro-PIXE. Applied Physics A 111, 69–74.

[17] Re, A., Lo Giudice, A.L., Angelici, D., Calusi, S., Giuntini, L., Massi, M., Pratesi, G., 2011. Lapis lazuli provenance study by means of micro-PIXE. Nuclear Instruments and Methods in Physics Research Section B: Beam Interactions with Materials and Atoms 269, 2373–2377.

[18] Lo Giudice A, Re A, Angelici D, Calusi S, Gelli N, Giuntini, L, Massi M, Pratesi M., 2012. In-air broad beam ionoluminescence microscopy as a tool for rocks and stone artworks characterisation. Anal Bioanal Chem 404(1):277–281.

[19] Da Cunha C., Le lapis lazuli: son histoire, ses gisements, ses imitations, Editions du Rucher, Paris

[20] Hogarth, D.D., Griffin, W.L., 1976. New data on lazurite. Lithos 9, 39–54.

[21] Brøgger, W.C., Bäckström, H., 1891. XII. Die Mineraliender Granatgruppe. Zeitschriftfür Kristallographie. Crystalline Materials, 18, 209–276.

[22] Hogarth, D.D., Griffin, W.L., 1980. Contact-metamorphic lapis lazuli; the Italian Mountain deposits, Colorado. The Canadian Mineralogist 18, 59–70.

[23] Coenraads, R.R., Canut de Bon, C., 2000. Lapis lazuli from the Coquimbo region, Chile. Gem. Gemol 36, 28–41.

[24] Cuitino, G.L., 1986. Mineralogía y génesis del yacimiento de lapislazuli, flor de los Andes, Coquimbo, Norte de Chile. Revista Geologica de Chile 57–67.

[25] Esquivela, R.C., Benavides Muñozc, M.E., 2005. Mineralogía y origen del yacimiento de lapislázuli Flor de los Andes, Chile. Boletín de Mineralogía 16, 57–65.

[26] Hogarth, D.D., Griffin, W.L., 1978. Lapis lazuli from Baffin Island—a Precambrian meta-evaporite. Lithos 11, 37–60.

[27] Moore, T.., Woodside, R.W., 2014. Sar-e-Sang The Mineralogical Record.

[28] Kievlenko, E.Y., 2003. Geology of gems. Ocean Pictures Ltd

[29] Petrakakis, K. and Dietrich, H., 1985. MINSORT: A program for the processing and archivation of microprobe analyses of silicate and oxide minerals. Neues Jahrbuch für Mineralogie, Mh. 8, 379-384.

[30] Fleet M. E. Liou X., Harmes S.L. and Nesbit H.W., 2005. Chemical state of Sulfur in natural and synthetic Lazurite by S K-Edge Xanes and X-ray photoelectronic spectroscopy. The Canadian Mineralogist, 43, 1589-1603.

[31] Whitney, D.L., Evans, B.W., 2010. Abbreviations for names of rock-forming minerals. American Mineralogist 95, 185–187.

[32] Aleksandrov S.M., Senin V.G., 2006. Genesis and composition of lazurite in magnesian skarns. Geochemistry International, 44(10): 976-988

[33] Morimoto N., 1988. "Nomenclature of Pyroxenes". Mineralogy and Petrology, 39: 55-76

[34] Holland, T.J.B., 1983. The Experimental Determination of Activities in Disordered and Short-Range Ordered Jadeitic Pyroxenes. 2, 41–52.

[35] Hawthorne, F.C., Oberti, R., Harlow, G.E., Maresch, W.V., Martin, R.F., Schumacher, J.C., Welch, M.D., 2012. Nomenclature of the amphibole supergroup. American Mineralogist 97, 2031–2048.

[36] Yurgenson G.A. & Sukharev B.P. 1985. Localization of lapis lazuli bodies of Badakhshan and their mineral zonation. International geology review, 27: 230-237

[37] Kostov 2004. Lazurite from central Asia according to the ethnonym Balkhara. Bulgarian Geological Society, Annual Scientific Conference, 38-40

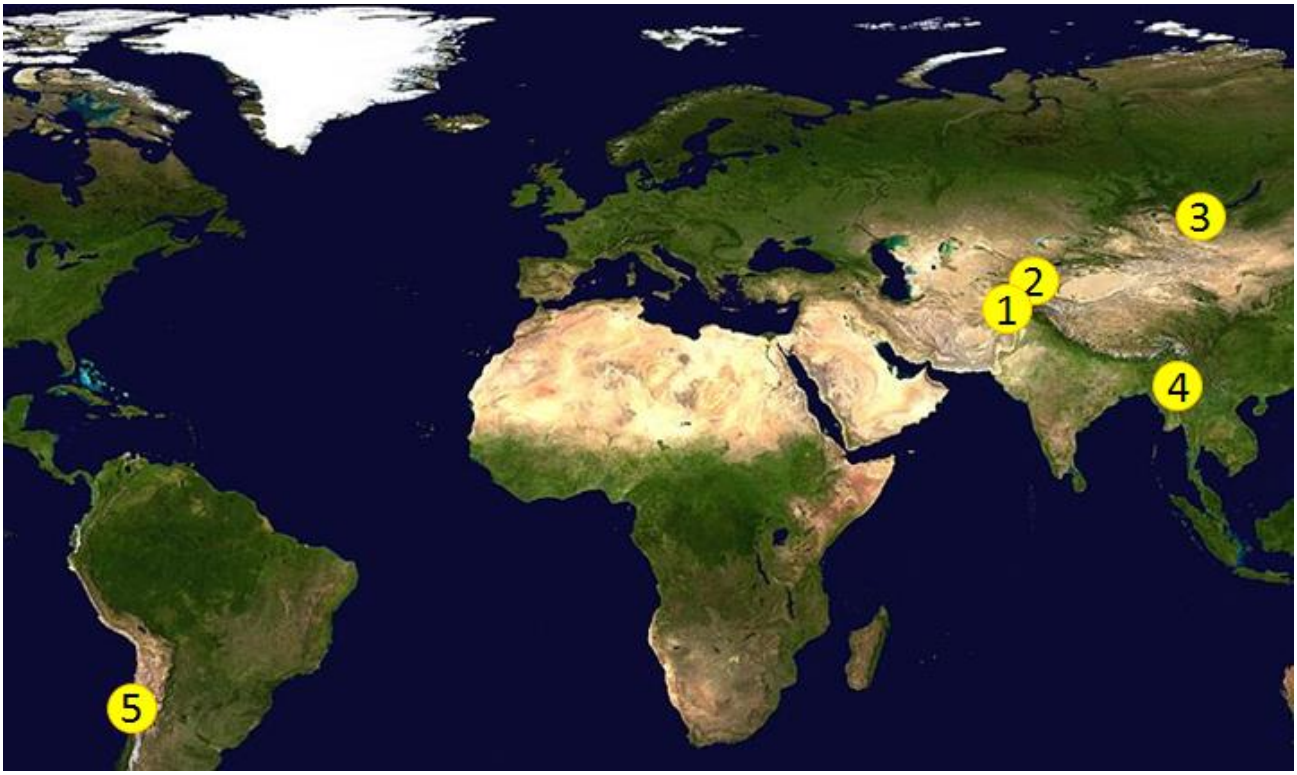

fig. 1

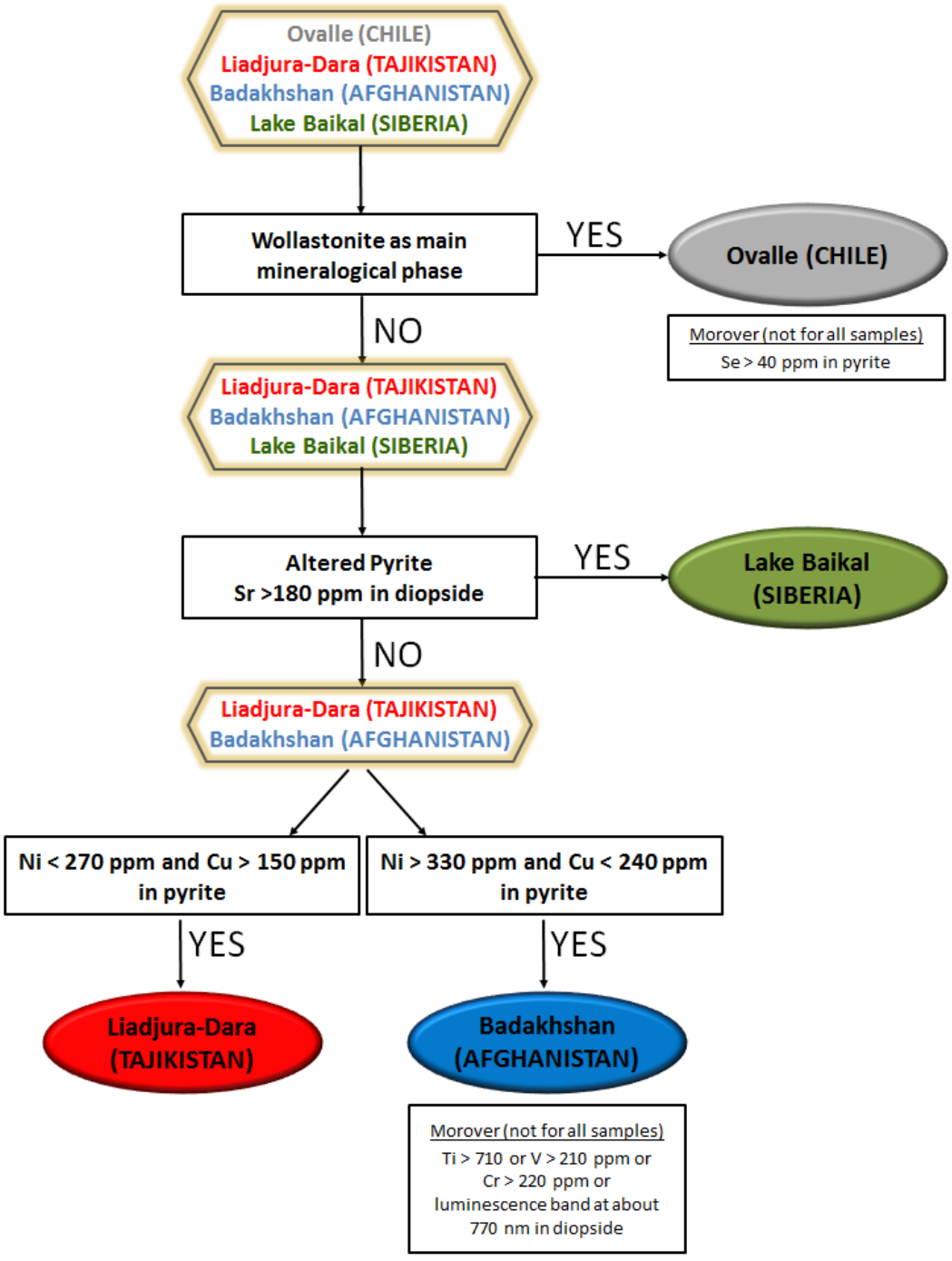
Ovalle (CHILE)
Liadjura-Dara (TAJIKISTAN)
Badakhshan (AFGHANISTAN)
Lake Baikal (SIBERIA)
Wollastonite as main mineralogical phase
YES
Ovalle (CHILE)
Morover (not for all samples)
Se > 40 ppm in pyrite
NO
Liadjura-Dara (TAJIKISTAN)
Badakhshan (AFGHANISTAN)
Lake Baikal (SIBERIA)
Altered Pyrite
Sr >180 ppm in diopside
YES
Lake Baikal (SIBERIA)
NO
Liadjura-Dara (TAJIKISTAN)
Badakhshan (AFGHANISTAN)
Ni < 270 ppm and Cu > 150 ppm in pyrite
Ni > 330 ppm and Cu < 240 ppm in pyrite
YES
YES
Liadjura-Dara (TAJIKISTAN)
Badakhshan (AFGHANISTAN)
Morover (not for all samples)
Ti > 710 or V > 210 ppm or
Cr > 220 ppm or
luminescence band at about
770 nm in diopside

fig. 2

fig. 3

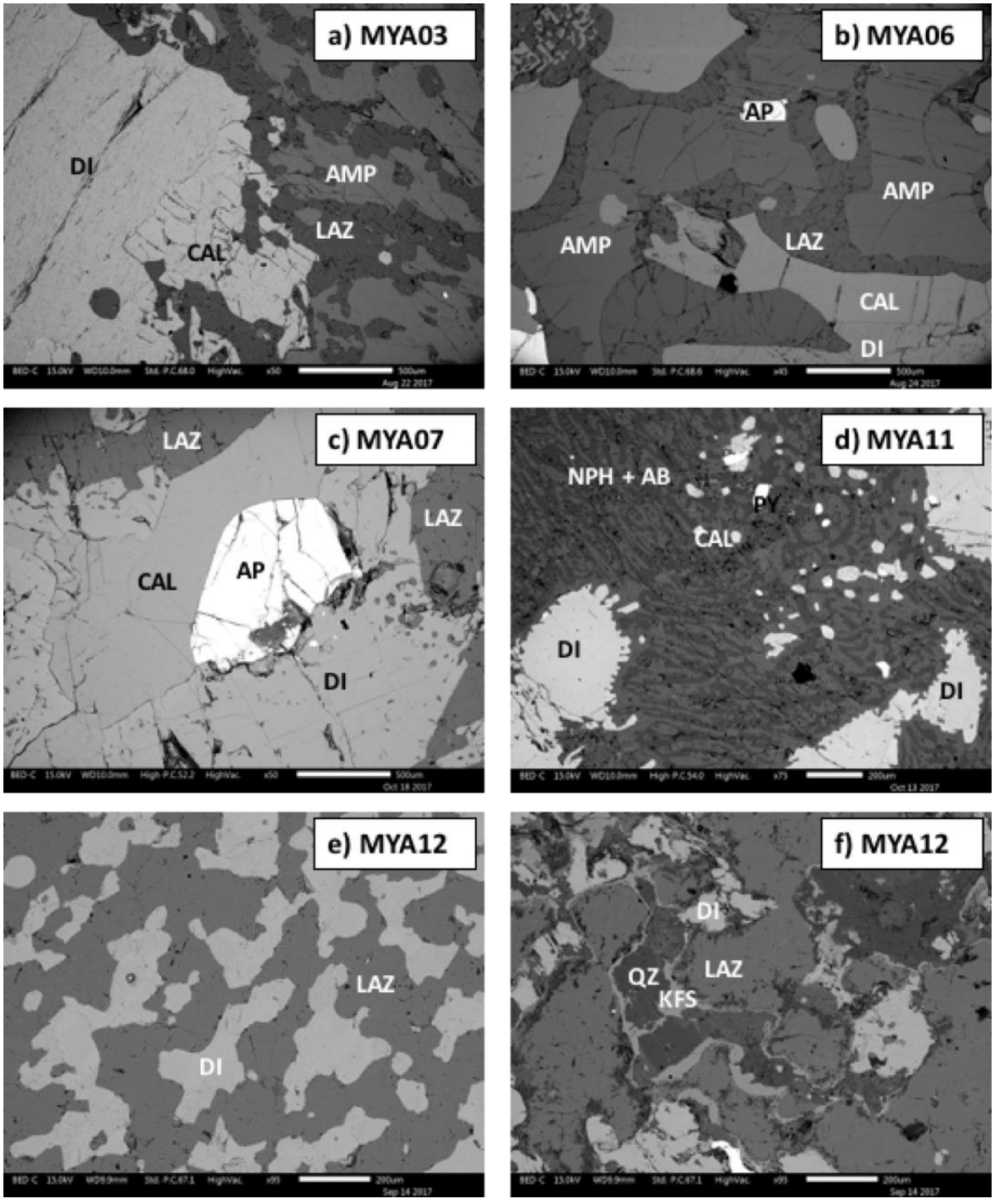
a) MYA03
DI
AMP
LAZ
CAL
b) MYA06
AP
AMP
AMP
LAZ
CAL
DI
c) MYA07
LAZ
LAZ
CAL
AP
DI
d) MYA11
NPH + AB
PY
CAL
DI
DI
e) MYA12
LAZ
DI
f) MYA12
DI
QZ
LAZ
KFS

fig. 4

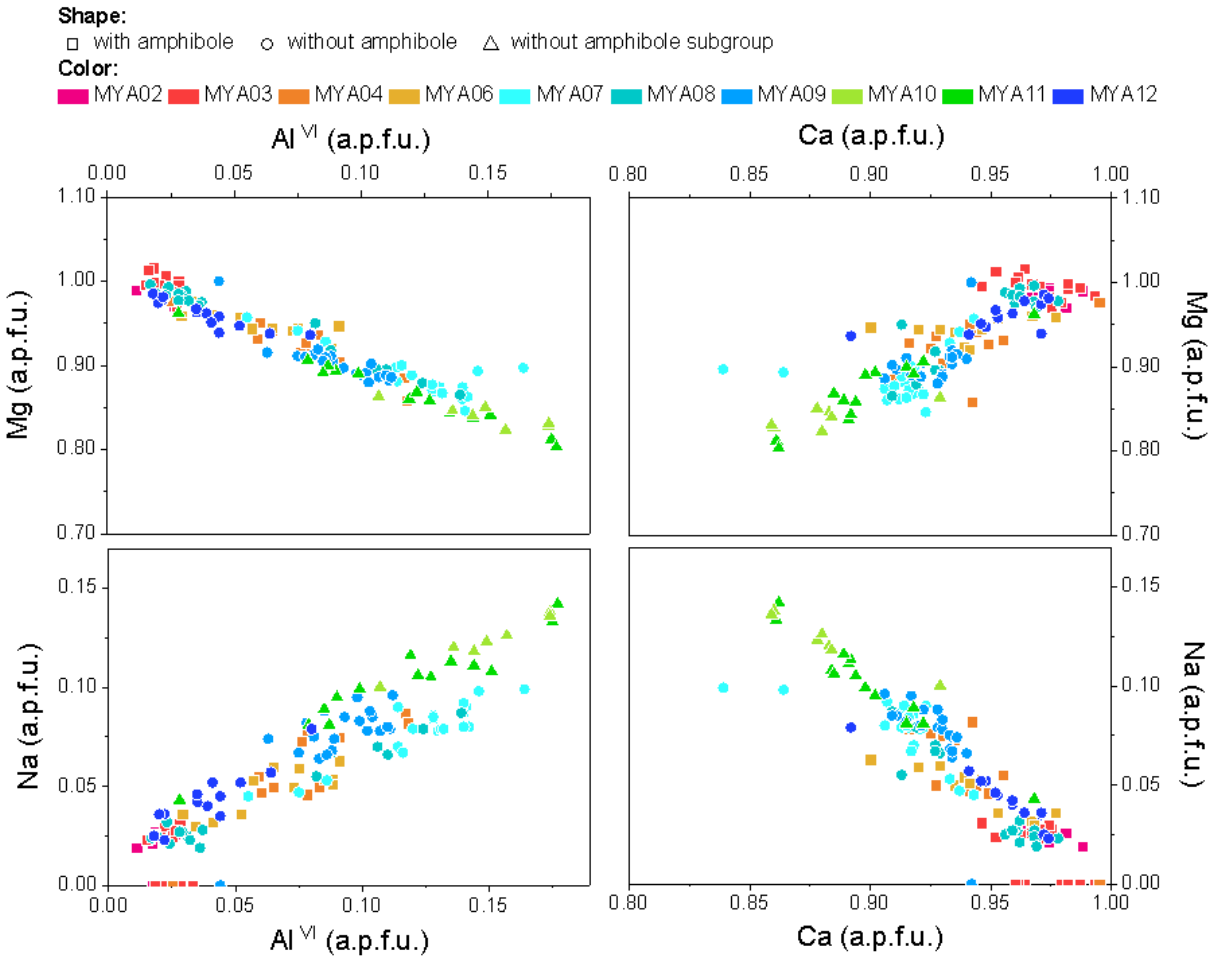
Shape:
with amphibole
without amphibole
without amphibole subgroup
Color:
MYA02
MYA03
MYA04
MYA06
MYA07
MYA08
MYA09
MYA10
MYA11
MYA12
Al VI (a.p.f.u.)
Ca (a.p.f.u.)
Mg (a.p.f.u.)
Na (a.p.f.u.)
0.00
0.05
0.10
0.15
0.80
0.85
0.90
0.95
1.00
0.70
0.80
0.90
1.00
1.10

fig. 5

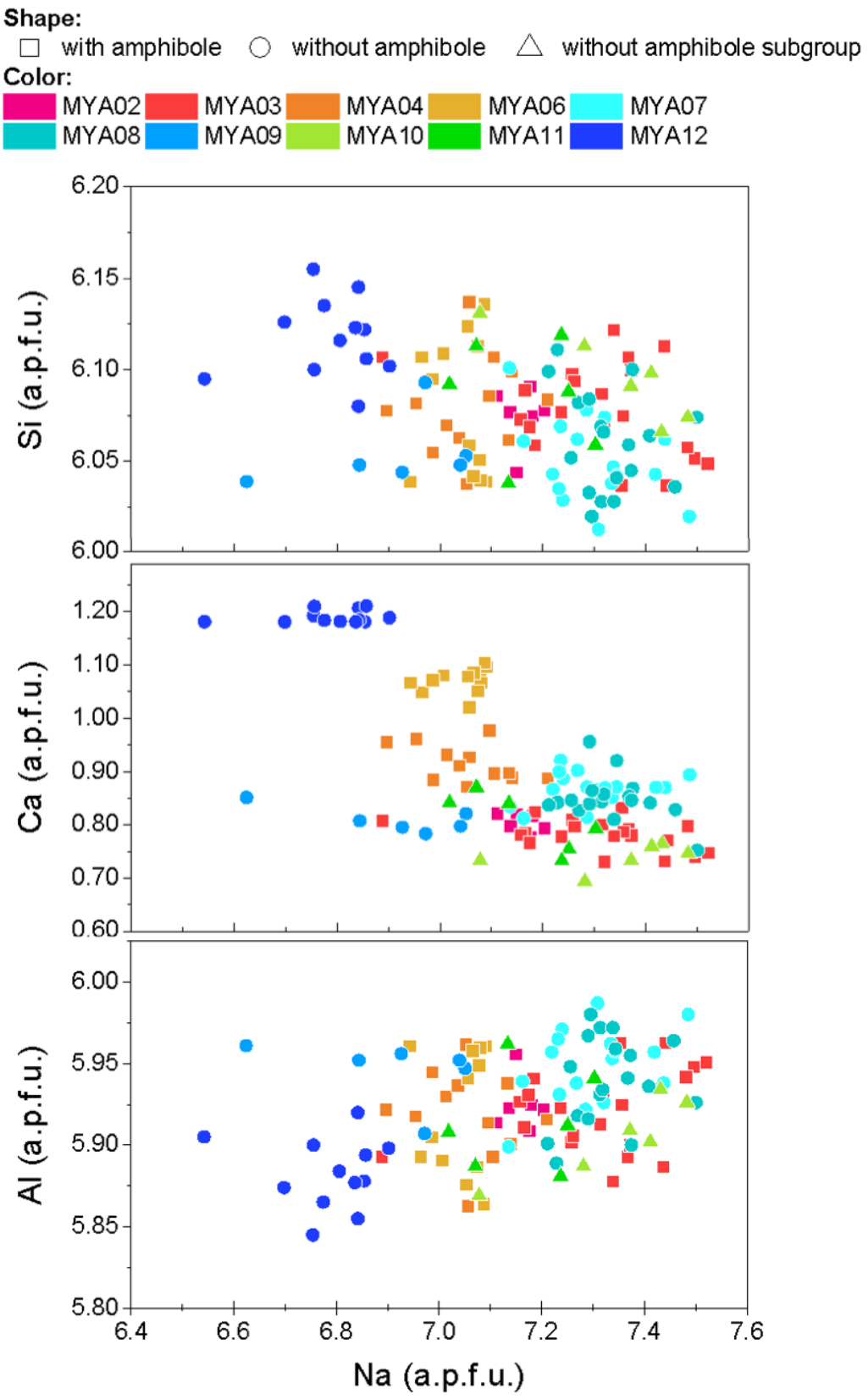
Shape:
with amphibole
without amphibole
without amphibole subgroup
Color:
MYA02
MYA03
MYA04
MYA06
MYA07
MYA08
MYA09
MYA10
MYA11
MYA12
Si (a.p.f.u.)
6.20
6.15
6.10
6.05
6.00
Ca (a.p.f.u.)
1.20
1.10
1.00
0.90
0.80
0.70
0.60
Al (a.p.f.u.)
6.00
5.95
5.90
5.85
5.80
6.4
6.6
6.8
7.0
7.2
7.4
7.6
Na (a.p.f.u.)

fig. 6

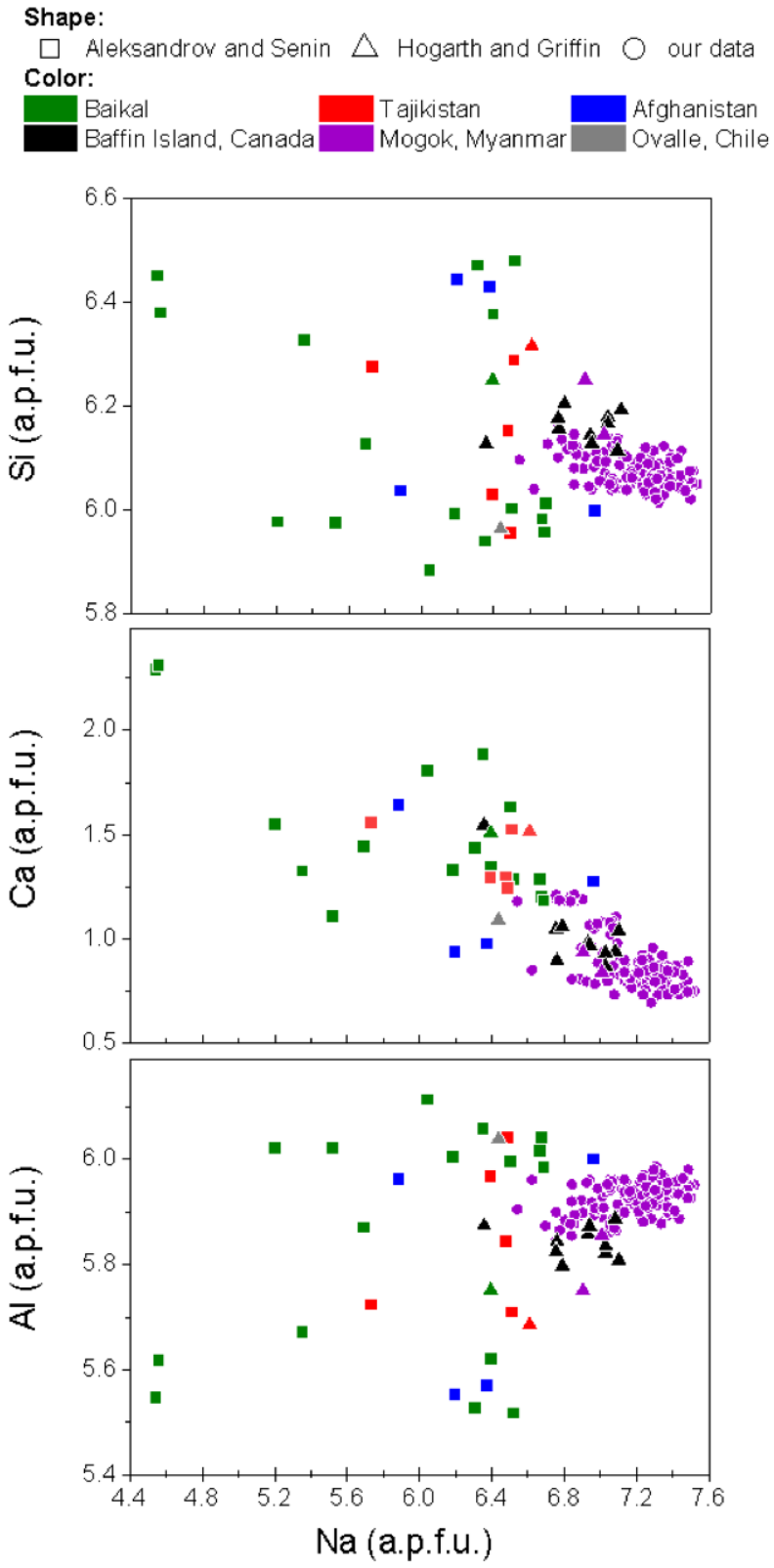
Shape:
Aleksandrov and Senin
Hogarth and Griffin
our data
Color:
Baikal
Tajikistan
Afghanistan
Baffin Island, Canada
Mogok, Myanmar
Ovalle, Chile
Si (a.p.f.u.)
Ca (a.p.f.u.)
Al (a.p.f.u.)
Na (a.p.f.u.)
6.6
6.4
6.2
6.0
5.8
2.0
1.5
1.0
0.5
6.0
5.8
5.6
5.4
4.4
4.8
5.2
5.6
6.0
6.4
6.8
7.2
7.6

fig. 7

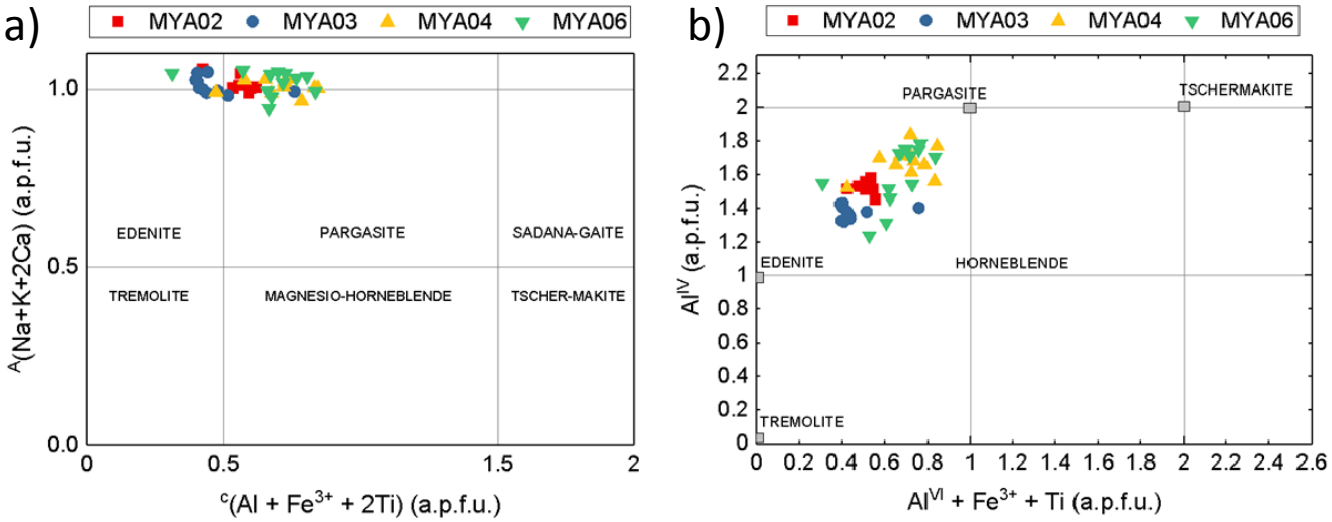
a)
MYA02
MYA03
MYA04
MYA06
EDENITE
PARGASITE
SADANA-GAITE
TREMOLITE
MAGNESIO-HORNEBLENDE
TSCHER-MAKITE
A(Na+K+2Ca) (a.p.f.u.)
C(Al + Fe3+ + 2Ti) (a.p.f.u.)
b)
MYA02
MYA03
MYA04
MYA06
PARGASITE
TSCHERMAKITE
EDENITE
HORNEBLENDE
TREMOLITE
AlIV (a.p.f.u.)
AlVI + Fe3+ + Ti (a.p.f.u.)

fig. 8

MINERALS		MYA02	MYA03	MYA04	MYA06	MYA07	MYA08	MYA09	MYA10	MYA11	MYA12
FELDSPHATOIDS	LAZURITE	x	x	x	x	x	x	x	x	x	x
	HAUYNE								x	x	
	NEPHELINE								x	x	
	SODALITE		x						x		
PYROXENES	DIOPSIDE	x	x	x	x	x	x	x	x	x	x
AMPHIBOLES	EDENITE-PARGASITE	x	x	x	x						
OPAQUE MINERALS	PYRITE	x	x	x	x		x	x	x	x	x
	Fe OXIDE-HYDROXIDE										x
MICAS	PHLOGOPITE									x	x
	MUSCOVITE										x
FELDSPAR	K-FELDSPAR										x
	PLAGIOCLASE								x	x	
	ALBITE								x	x	
OTHERS	CALCITE	x	x	x	x	x	x	x	x	x	
	DOLOMITE										x
	APATITE	x	x	x		x	x	x	x	x	x
	KAOLINITE							x			
	SCAPOLITE								x		
	CORDIERITE										X
	QUARTZ										x
	PITCHBLENDE		x	x		x	x	x			x
SULFIDES	CHALCOCITE						x				
	SPHALERITE						x				

Table 1

	MYA02		MYA04		MYA06		MYA07		MYA08		MYA11	
SiO_2	55.01	55.22	54.32	54.86	54.53	54.70	54.43	54.93	55.30	53.71	54.76	54.58
TiO_2	bdl	bdl	bdl	bdl	bdl	bdl	bdl	bdl	bdl	bdl	bdl	bdl
Al_2O_3	0.90	0.70	3.98	2.48	2.42	1.61	4.41	2.45	1.17	5.15	2.74	4.09
Cr_2O_3	bdl	bdl	bdl	bdl	bdl	bdl	bdl	bdl	bdl	bdl	bdl	bdl
FeO	bdl	bdl	bdl	bdl	bdl	bdl	bdl	bdl	bdl	bdl	0.44	0.54
MnO	bdl	bdl	bdl	bdl	bdl	bdl	bdl	bdl	bdl	bdl	bdl	bdl
MgO	18.60	18.53	16.57	17.68	17.66	18.33	16.08	18.06	18.21	16.22	16.95	16.08
CaO	25.38	25.55	23.65	24.65	24.62	25.25	23.58	24.75	24.93	23.71	23.99	23.32
Na_2O	0.33	0.00	1.25	0.72	0.76	0.43	1.32	0.65	0.40	1.25	1.16	1.51
Total	100.22	100.00	99.78	100.38	99.99	100.32	99.83	100.84	99.99	100.04	100.04	100.12
Si	1.97	1.99	1.95	1.96	1.96	1.96	1.95	1.95	1.99	1.92	1.96	1.95
Al IV	0.03	0.01	0.05	0.04	0.05	0.04	0.05	0.05	0.01	0.08	0.04	0.05
Al VI	0.01	0.02	0.12	0.07	0.06	0.03	0.14	0.06	0.04	0.14	0.08	0.13
Fe 3+	-	-	-	-	-	-	-	-	-	-	0.04	0.02
Mg	0.99	0.98	0.88	0.94	0.94	0.98	0.86	0.94	0.96	0.86	0.91	0.86
Fe 2+	-	-	-	-	-	-	-	-	-	-	-	-
Mg	0.00	0.01	0.00	0.01	0.00	0.00	0.00	0.01	0.01	0.00	0.00	0.00
Ca	0.97	0.99	0.91	0.94	0.95	0.97	0.91	0.94	0.96	0.91	0.92	0.89
Na	0.02	0.00	0.09	0.05	0.05	0.03	0.09	0.05	0.03	0.09	0.08	0.11
jd	0.02	0.00	0.07	0.03	0.01	0.03	0.09	0.01	0.03	0.06	0.04	0.08
fs	0.00	0.00	0.00	0.00	0.00	0.00	0.00	0.00	0.00	0.00	0.01	0.01
en	0.50	0.50	0.44	0.47	0.47	0.49	0.43	0.48	0.49	0.43	0.45	0.43
wo	0.47	0.49	0.43	0.45	0.45	0.46	0.43	0.45	0.47	0.42	0.44	0.42

Table 2

	MYA02		MYA04		MYA06		MYA07		MYA08		MYA11	
SiO_2	33.03	33.44	32.82	32.69	33.53	33.62	32.02	31.85	32.36	32.10	31.09	31.53
Al_2O_3	27.23	27.65	27.50	27.23	27.45	27.63	27.05	26.71	26.78	26.99	26.04	25.98
CaO	4.16	4.10	4.42	4.46	5.38	5.52	4.30	4.43	3.74	4.19	4.04	3.64
Na_2O	19.91	20.25	19.77	19.45	19.72	19.87	20.07	19.69	20.61	20.09	18.94	19.37
K_2O	0.25	0.37	0.33	0.41	0.00	0.00	0.12	0.15	0.22	0.13	0.33	0.58
SO_3	14.17	13.54	14.32	14.80	13.48	13.08	14.93	15.59	14.59	14.92	17.38	16.93
Cl	0.44	0.00	0.00	0.00	0.00	0.00	0.69	0.61	0.97	0.73	0.58	0.54
S	0.17	0.12	0.17	0.20	0.12	0.10	0.07	0.10	0.08	0.08	0.27	0.24
Σ	99.35	99.47	99.33	99.23	99.68	99.80	99.23	99.11	99.35	99.23	98.68	98.80
Si	6.09	6.08	6.04	6.06	6.11	6.10	6.01	6.04	6.07	6.03	6.04	6.09
Al	5.91	5.92	5.96	5.95	5.89	5.91	5.99	5.97	5.93	5.97	5.96	5.91
Σ	12.00	12.00	12.00	12.00	12.00	12.00	12.00	12.00	12.00	12.00	12.00	12.00
Ca	0.82	0.80	0.87	0.89	1.05	1.07	0.87	0.90	0.75	0.84	0.84	0.75
Na	7.11	7.14	7.05	6.99	6.96	6.99	7.31	7.23	7.50	7.32	7.13	7.25
K	0.06	0.09	0.08	0.10	0.00	0.00	0.03	0.04	0.05	0.03	0.08	0.14
Σ	7.99	8.02	8.00	7.97	8.01	8.06	8.20	8.17	8.31	8.19	8.06	8.06
SO_4	1.96	1.85	1.98	2.06	1.84	1.78	2.10	2.22	2.06	2.10	2.53	2.45
Cl	0.14	0.00	0.00	0.00	0.00	0.00	0.22	0.20	0.31	0.23	0.19	0.18
Σ	2.10	1.85	1.98	2.06	1.84	1.78	2.32	2.41	2.36	2.33	2.72	2.72
S	0.06	0.04	0.06	0.07	0.04	0.03	0.02	0.03	0.03	0.03	0.10	0.09
O	23.94	23.96	23.94	23.93	23.96	23.97	23.98	23.97	23.97	23.97	23.90	23.91
Σ	24.00	24.00	24.00	24.00	24.00	24.00	24.00	24.00	24.00	24.00	24.00	24.00

Table 3

	MYA2			MYA3			MYA4			MYA6		
SiO_2	46.55	47.33	46.40	47.67	47.44	48.12	45.01	44.63	45.05	46.65	45.06	45.12
TiO_2	0.71	0.54	0.43	0.00	0.00	0.00	0.00	0.00	0.00	0.48	0.44	0.00
Al_2O_3	12.47	11.52	12.00	11.79	10.86	10.90	15.96	16.48	14.75	12.98	15.33	14.79
Cr_2O_3	bdl	bdl	bdl	bdl	bdl	bdl	bdl	bdl	bdl	bdl	bdl	bdl
FeO	bdl	bld	bdl	bdl	bld	bdl	bdl	bld	bdl	bdl	bld	bdl
MgO	21.54	21.97	21.53	21.73	22.13	22.08	20.25	20.32	20.51	21.19	20.61	20.71
CaO	13.17	12.96	13.10	12.94	12.91	12.94	13.00	13.31	12.85	12.72	13.18	13.36
Na_2O	3.70	3.77	3.56	3.69	3.81	3.72	3.70	3.40	3.71	3.73	3.64	3.53
K_2O	0.42	0.41	0.53	0.46	0.45	0.44	0.43	0.56	0.48	0.49	0.68	0.67
Total	98.57	98.49	97.55	98.28	97.59	98.20	98.34	98.69	97.37	98.25	98.95	98.19
Si	6.44	6.54	6.48	6.59	6.62	6.66	6.23	6.16	6.30	6.46	6.22	6.27
Al^{IV}	1.56	1.46	1.52	1.41	1.38	1.34	1.77	1.84	1.70	1.54	1.78	1.73
Al^{VI}	0.47	0.42	0.46	0.52	0.40	0.44	0.83	0.84	0.73	0.58	0.71	0.70
Ti	0.07	0.06	0.05	0.00	0.00	0.00	0.00	0.00	0.00	0.05	0.05	0.00
Cr	-	-	-	-	-	-	-	-	-	-	-	-
Fe^{3+}	-	-	-	-	-	-	-	-	-	-	-	-
Mg	4.44	4.53	4.49	4.48	4.60	4.56	4.18	4.18	4.28	4.38	4.24	4.29
Fe^{2+}	-	-	-	-	-	-	-	-	-	-	-	-
Ca	1.95	1.92	1.96	1.92	1.93	1.92	1.93	1.97	1.93	1.89	1.95	1.99
Na	0.06	0.08	0.05	0.09	0.07	0.09	0.06	0.03	0.06	0.11	0.06	0.02
Na	0.93	0.93	0.92	0.90	0.97	0.91	0.93	0.90	0.94	0.89	0.92	0.93
K	0.08	0.07	0.10	0.08	0.08	0.08	0.08	0.10	0.09	0.09	0.12	0.12

Table 4

	MYA10			MYA11			MYA12	
	PLG		ALB	PLG		ALB	K-FELD	
SiO_2	63.84	63.43	65.62	62.46	66.07	65.96	66.06	65.18
Al_2O_3	22.62	22.75	21.23	22.94	21.30	21.00	18.72	18.87
CaO	3.65	3.90	2.08	4.51	2.13	1.97	bdl	bdl
Na_2O	9.78	9.50	10.86	9.32	10.90	10.81	1.98	1.91
K_2O	0.00	0.07	0.08	0.14	0.04	0.18	14.04	13.90
Total	99.89	99.65	99.86	99.37	100.43	99.92	100.80	99.86
Al	1.18	1.19	1.10	1.21	1.10	1.09	1.00	1.02
Si	2.82	2.81	2.89	2.78	2.89	2.90	3.00	2.99
Ca	0.17	0.19	0.09	0.22	0.10	0.09	-	-
Na	0.84	0.82	0.93	0.81	0.93	0.92	0.17	0.17
K	0.00	0.00	0.00	0.01	0.00	0.01	0.81	0.81

Table 5